

# Easily tunable nonlinear optical loop mirror based on polarization asymmetry

O. Pottiez<sup>1,2</sup>, E. A. Kuzin<sup>2</sup>, B. Ibarra-Escamilla<sup>2</sup>, J. T. Camas-Anzueto<sup>2</sup> and F. Gutiérrez-Zainos<sup>2</sup>

<sup>1</sup>Postdoctoral Researcher of F.N.R.S., Service d'Electromagnétisme et de Télécommunications, Faculté Polytechnique de Mons, Bd Dolez 31, 7000 Mons, Belgium  
[pottiez@telecom.fpms.ac.be](mailto:pottiez@telecom.fpms.ac.be)

<sup>2</sup>Instituto Nacional de Astrofísica, Óptica y Electrónica, L. E. Erro 1, 72840 Puebla, Mexico

**Abstract:** The operation of an unconventional, power-symmetric nonlinear optical loop mirror (NOLM) is investigated. Its principle is based on the creation of a polarization asymmetry between the counterpropagating beams, through the use of a quarter-wave plate and highly twisted fiber in the loop. Using a very intuitive approach, we propose a simple although comprehensive description of the NOLM operation. By adjusting the angle of the quarter-wave plate, the interferometer can be tuned continuously from non-power-dependent operation to nonlinear switching, in a very convenient way. Experimental results confirm theoretical predictions. The properties of the proposed NOLM design make it very attractive for various applications, like pedestal suppression and amplitude regularization of optical pulse trains.

©2004 Optical Society of America

**OCIS codes:** (230.4320) Nonlinear optical devices; (060.4370) Nonlinear optics, fibers; (190.3270) Kerr effect; (230.5440) Polarization-sensitive devices; (060.2330) Fiber optics communications.

---

## References and links

1. A. E. Siegman, "An antiresonant ring interferometer for coupled laser cavities, laser output coupling, mode locking, and cavity dumping," *IEEE J. Quantum Electron.* **QE-9**, 247-250 (1973).
2. D. B. Mortimore, "Fiber loop reflectors," *J. Lightwave Technol.* **6**, 1217-1224 (1988).
3. Y. W. Lee, J. Jung, and B. Lee, "Multiwavelength-switchable SOA-fiber ring laser based on polarization-maintaining fiber loop mirror and polarization beam splitter," *IEEE Photon. Technol. Lett.* **16**, 54-56 (2004).
4. E. A. Kuzin, J. M. Estudillo-Ayala, B. Ibarra-Escamilla, and J. W. Haus, "Measurements of beat length in short low-birefringence fibers," *Opt. Lett.* **26**, 1134-1136 (2001).
5. E. Simova and I. Golub, "Phase-stepping an all-fiber Sagnac loop for full characterization of femtosecond PMD," *IEEE Photon. Technol. Lett.* **15**, 960-962 (2003).
6. K. Mori, T. Morioka, and M. Saruwatari, "Optical parametric loop mirror," *Opt. Lett.* **20**, 1424-1426 (1995).
7. H. C. Lim, F. Futami, and K. Kikuchi, "Polarization-independent, wavelength-shift-free optical phase conjugator using a nonlinear fiber Sagnac interferometer," *IEEE Photon. Technol. Lett.* **11**, 578-580 (1999).
8. N. J. Doran and D. Wood, "Nonlinear optical loop mirror," *Opt. Lett.* **13**, 56-58 (1988).
9. H. Sotobayashi, C. Sawaguchi, Y. Koyamada, and W. Chujo, "Ultrafast walk-off-free nonlinear optical loop mirror by a simplified configuration for 320-Gbit/s time-division multiplexing signal demultiplexing," *Opt. Lett.* **27**, 1555-1557 (2002).
10. W. W. Tang, C. Shu, and K. L. Lee, "Rational harmonic mode locking of an optically triggered fiber laser incorporating a nonlinear optical loop modulator," *IEEE Photon. Technol. Lett.* **13**, 16-18 (2001).
11. I. N. Duling III, "All-fiber ring soliton laser mode locked with a nonlinear mirror," *Opt. Lett.* **16**, 539-541 (1991).
12. M. D. Pelusi, Y. Matsui, and A. Suzuki, "Pedestal suppression from compressed femtosecond pulses using a nonlinear fiber loop mirror," *IEEE J. Quantum Electron.* **35**, 867-874 (1999).

13. M. Attygalle, A. Nirmalathas, and H. F. Liu, "Novel technique for reduction of amplitude modulation of pulse trains generated by subharmonic synchronous mode-locked laser," *IEEE Photon. Technol. Lett.* **14**, 543-545 (2002).
14. A. Bogoni, P. Ghelfi, M. Scaffardi, and L. Poti, "All-optical regeneration and demultiplexing for 160-Gb/s transmission systems using a NOLM-based three-stage scheme," *IEEE J. Sel. Top. Quantum Electron.* **10**, 192-196 (2004).
15. J. D. Moores, K. Bergman, H. A. Haus, and E. P. Ippen, "Optical switching using fiber ring reflectors," *J. Opt. Soc. Am. B* **8**, 594-601 (1991).
16. W. S. Wong, S. Namiki, M. Margalit, H. A. Haus, and E. P. Ippen, "Self-switching of optical pulses in dispersion-imbalanced nonlinear loop mirrors," *Opt. Lett.* **22**, 1150-1152 (1997).
17. E. A. Kuzin, N. Korneev, J. W. Haus, and B. Ibarra-Escamilla, "Theory of nonlinear loop mirrors with twisted low-birefringence fiber," *J. Opt. Soc. Am. B* **18**, 919-925 (2001).
18. S. F. Feldman, D. A. Weinberger, and H. G. Winful, "Polarization instability in a twisted birefringent optical fiber," *J. Opt. Soc. Am. B* **10**, 1191-1201 (1993).
19. O. Pottiez, E. A. Kuzin, B. Ibarra-Escamilla, and F. Méndez Martínez, "Easily tuneable nonlinear optical loop mirror including low-birefringence, highly twisted fibre with invariant output polarisation," *Opt. Commun.* **229**, 147-159 (2004).
20. O. Pottiez, E. A. Kuzin, B. Ibarra-Escamilla, J. T. Camas-Anzueto, and F. Gutiérrez-Zainos, "Experimental demonstration of NOLM switching based on nonlinear polarisation rotation," *Electron. Lett.* **40**, 892-894 (2004).
21. Y. Liang, J. W. Lou, J. K. Andersen, J. C. Stocker, O. Boyraz, M. N. Islam, and D. A. Nolan, "Polarization-insensitive nonlinear optical loop mirror demultiplexer with twisted fiber," *Opt. Lett.* **24**, 726-728 (1999).
22. H. C. Lefevre, "Single-mode fibre fractional wave devices and polarisation controllers," *Electron. Lett.* **16**, 778-780 (1980).

## 1. Introduction

When the concept of a Sagnac interferometer (SI) first emerged in the laser world, it was already opening the way for several promising applications [1]. With the passage of time, its appeal for the laser community has not diminished. Indeed, its design, in which two interfering signals counter-propagate along the same optical path, is very simple, making the SI very robust to external perturbations. Moreover, its implementation in fiber optics technology, using a directional coupler whose output ports are connected to form a loop, is extremely straightforward. Basically, the device is a mirror, but its reflectivity strongly depends on the loop birefringence [2], a property that is now exploited to realize variable optical filters [3], or for the measurement of low birefringence [4] or polarization-mode dispersion [5] in optical fibers. In the field of nonlinear optics, the fiber SI proved to be useful for four-wave mixing applications [6], in particular optical phase conjugation [7], but it is its power-dependent reflection (or transmission) characteristic, due to the optical Kerr effect, that received most attention.

The fiber SI, in this case called a Nonlinear Optical Loop Mirror (NOLM) [8], is now commonly used for applications like optical switching and demultiplexing [9], all-optical active mode locking [10], passive mode locking [11], pedestal suppression [12], amplitude regularization of optical pulse trains [13] or regeneration of ultrafast data streams [14]. Indeed, adjusting the control optical power (either the input signal itself, or a pump beam), the interferometer can be switched from a highly reflective to a transparent state (or conversely), provided that a nonlinear phase shift difference appears between the clockwise (CW) and counter-clockwise (CCW) signal beams. When the control is the signal itself, this condition is readily obtained by creating a power imbalance between the CW and CCW beams, usually through the use of an asymmetric coupler in the NOLM design [8], or by inserting some loss (or gain) after one of the coupler output ports [12-14]. With these designs however, it is difficult to conciliate high contrast with low critical power and low insertion loss (except of course if gain is used). For signals made of short pulses, an asymmetry in the loop birefringence [15] or dispersion [16] also proved to be efficient. In these cases, the power imbalance is obtained by splitting or stretching the pulses in the loop, in such a way that their peak power undergoes different evolutions in CW and CCW directions. These structures are more complex however, and impose more stringent requirements on the fiber used in the loop.

In spite of the extreme diversity of the NOLM architectures that were proposed, a feature that is common to all these schemes is the existence of a power asymmetry between the counterpropagating beams. The classical model [8] shows indeed that this condition is required to obtain switching. On the other hand, the impact of nonlinear polarization effects on the NOLM operation was practically never considered, until Kuzin *et al.* finally addressed the problem in a comprehensive way [17]. Using a model including the general coupled equations for nonlinear polarization evolution in the continuous-wave case [18], these authors demonstrated the crucial importance of a vectorial approach to accurately describe the NOLM behavior. As a matter of fact, similarly to a power imbalance, a polarization asymmetry between the counterpropagating beams can provide a nonlinear phase difference and, thereby, switching.

In a previous publication [19], we used this model to detail the operation of a particular NOLM configuration, including highly twisted fiber and a quarter-wave plate (QWP) in the loop, in the case of circular input polarization. We found in particular that, if the NOLM is power-symmetric (when a symmetrical coupler is used), an optimal switching behavior is obtained, which relies exclusively on the polarization asymmetry generated by the QWP. Recently, we demonstrated experimentally that switching with very high contrast can be obtained using this set-up, for a proper adjustment of the QWP angle, and that this switching relies on nonlinear polarization evolution [20]. In this Paper, we first propose a simple, intuitive description of the NOLM operation, yielding results compatible with Ref. 19, and which shows that the validity of this simple model strongly depends on the actual polarization states of the beams that propagate in the loop. We then characterize experimentally the NOLM transmission for several values of the QWP angle. In all cases, these experimental results are in good agreement with the predictions, which clearly demonstrates that the model is valid in real experimental conditions.

## 2. Description of NOLM operation

To understand how two beams with equal powers can undergo a nonlinear phase difference let us consider the coupled nonlinear equations [18]:

$$\begin{aligned}\partial_z C^+ &= i\beta P \left( |C^+|^2 + 2|C^-|^2 \right) C^+; \\ \partial_z C^- &= i\beta P \left( |C^-|^2 + 2|C^+|^2 \right) C^-, \end{aligned} \quad (1)$$

where  $\partial_z$  denotes the first derivative with respect to the direction of propagation  $z$ ,  $\beta = 4\tilde{n}_2 / (3\lambda A_{\text{eff}})$  is the nonlinearity coefficient ( $\tilde{n}_2$  being the Kerr coefficient,  $\lambda$  the wavelength and  $A_{\text{eff}}$  the effective modal area),  $P$  is the beam power, and  $C^+$  and  $C^-$  are the complex amplitudes of the circular right and left polarization components, respectively, normalized to the power, in such a way that  $|C^+|^2 + |C^-|^2 = 1$ . In the right-hand sides of Eq. (1), we omitted the linear terms, which account for linear and circular birefringence (optical activity). These equations describe the nonlinear phase evolution of each polarization component, which is governed not only by its own magnitude (self-phase modulation), but also by the magnitude of the complementary polarization component (cross-phase modulation). Considering two beams at the same wavelength, propagating in the same medium, a nonlinear phase difference may appear between them, according to Eq. (1), either if their powers are different, or if they have different polarizations. To illustrate the latter case, let us consider two beams having the same power  $P$ , but with circular (left or right) and linear polarizations, respectively. Integrating Eq. (1) along a length  $L$  in both cases, we obtain easily the nonlinear phase shifts  $\varphi_{NL,c} = \beta PL$  for the circularly polarized beam, and  $\varphi_{NL,l} = 3/2\beta PL$  for the linearly polarized one. For these polarizations, the nonlinear phase

difference  $\Delta\varphi_{NL} = |\varphi_{NL,l} - \Delta\varphi_{NL,c}| = \beta PL/2$  is maximal (considering beams of equal power). Note also that, with an exception in the case of linear polarization ( $|C^+|^2 = |C^-|^2 = 1/2$ ), the nonzero difference between the nonlinear coefficients  $|C^+|^2 + 2|C^-|^2$  and  $|C^-|^2 + 2|C^+|^2$  that appear in Eq. (1) causes a nonlinear polarization rotation (NPR), which is maximal for circularly polarized light (although it is not apparent in this case, a circle being transformed into itself after rotation).

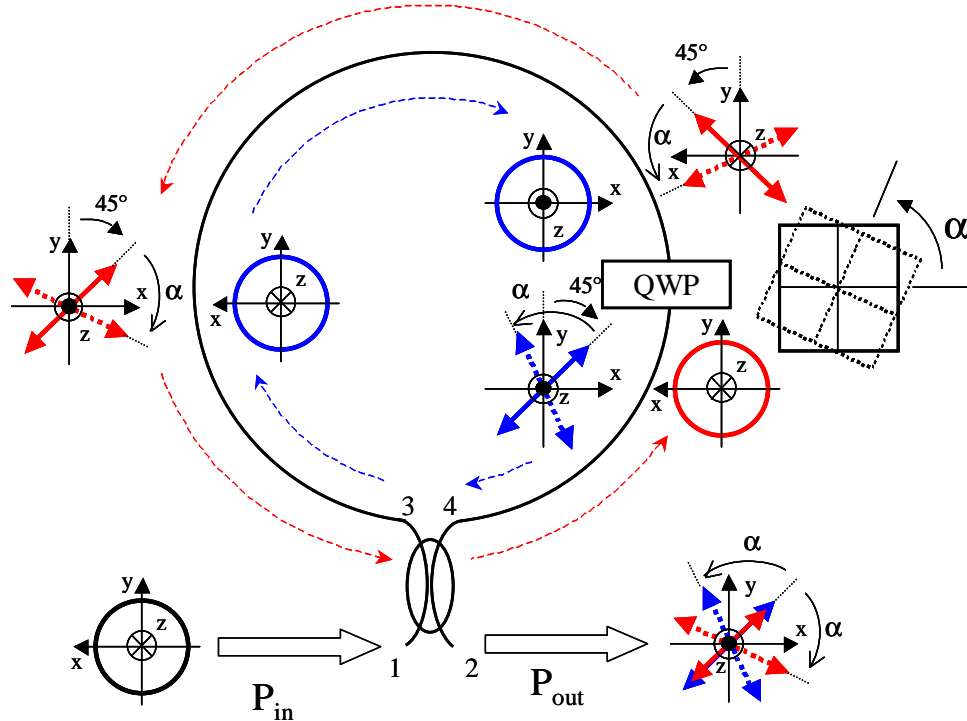


Fig. 1. Schematic representation of the polarization evolution in the NOLM under study, for circular input polarization. The  $z$  axis corresponds to the propagation direction. The effect of the twist-induced optical activity of the loop was not represented. Solid lines correspond to the initial position of the QWP ( $\alpha = 0$ ), and dotted lines to the QWP rotated by an angle  $\alpha$ .

The NOLM that we consider here is similar to the one described in Ref. 20. It is made of a symmetrical coupler, a piece of standard, highly twisted fiber connecting the coupler output ports, and a QWP inserted in the loop, close to one of the coupler outputs. Due to the asymmetrical location of the QWP in the loop, the CW and CCW beams propagate in the loop with different polarization states. For this purpose, the high twist applied to the fiber also is crucial. Indeed, it generates a strong optical activity (or circular birefringence) along the fiber, which takes over its residual (linear and circular) birefringence, and ensures that the polarization states will not be modified during propagation (except for a rotation). In addition to optical activity, twist also generates a rapid precession of the fiber principal axes, which for purely geometrical reasons tends to cancel the effect of linear birefringence [18]. This polarization-preserving condition is important in practice, as the existence of a nonlinear phase difference  $\Delta\varphi_{NL} = \beta PL/2$  between the counterpropagating beams supposes that their polarizations are maintained during propagation along a length  $L$  of the fiber. In contrast, in the case of conventional (power-asymmetric) NOLMs made of untwisted standard fiber,

although a polarization asymmetry can be generated by the use of a polarization controller in the loop, the polarization states of the beams are not maintained along the loop, and evolve quite randomly during propagation, as a result of both intrinsic and externally induced birefringence. As a consequence, the nonlinear phase difference generated by the polarization asymmetry tends to vanish. Hence, nonlinear polarization effects are likely to have little influence on the switching of conventional NOLMs. This might be the reason why such effects are practically never considered for the description of NOLM operation. Note finally that twist was already shown to be useful in a NOLM, allowing to perform polarization-insensitive demultiplexing [21].

In the description that we propose in the following, dealing with the continuous-wave case, we neglect the group velocity mismatch that appears in a twisted fiber between the two circular polarization components. Considering a pulsed signal, this approximation is valid, strictly speaking, as far as  $\delta L \ll T_0$ , where  $\delta = \Delta n / c$  is the delay per unit length between  $C^+$  and  $C^-$  components ( $\Delta n = |n_- - n_+|$  is the refractive index mismatch and  $c$  the speed of light in vacuum),  $L$  is the fiber length and  $T_0$  the pulse duration. In the case of picosecond pulses, which are used in ultrafast photonics systems, some deviation with respect to the ideal case has to be expected, especially when long fiber lengths and very high twist (high  $\delta$ ) are used. Hence, care has to be taken while designing a NOLM for a particular application, that the group velocity mismatch remain limited, so that it will not degrade seriously the NOLM performances.

The operation of the proposed NOLM architecture can be described in a very simple way when the input polarization state is circular (Fig. 1). If the input beam is circularly polarized, the symmetrical coupler divides it into two beams with equal power and circular polarization, which start to propagate in the loop in CW and CCW directions, respectively. Because of the location of the QWP close to the coupler port 4, the CW beam has during propagation a circular polarization, which is maintained by the strong optical activity of the fiber. After propagation through the loop, the circular polarization is turned into a linear polarization making an angle of  $45^\circ$  with the QWP principal axes (say, to the left with respect to the vertical axis). In the case of the CCW beam, the circular polarization is first turned into linear polarization, with an angle of  $45^\circ$  with the QWP principal axes, in the same direction as the CW beam, i.e., to the left relatively to this direction of propagation. This linearly polarized beam then propagates in the loop. Through the loop, because of optical activity, the polarization state is rotated, but remains linear. The NOLM output is thus obtained by the combination of two linearly polarized beams. Nevertheless, as during propagation in the loop, the CW beam is circularly polarized, whereas the CCW beam is linearly polarized, they accumulate a nonlinear phase shift difference.

Let us first consider that the QWP angle  $\alpha$  is such that the linear polarizations at the NOLM output are parallel, so that they may interfere (we take  $\alpha = 0$  in this case). Due to the coupler, a phase difference  $\Delta\phi_L = \pi$  exists between the CW and CCW beams, so that in the linear regime (at low power), interference is destructive and, as both fields have equal amplitudes, NOLM transmission is zero. In the nonlinear regime, a nonlinear phase difference  $\Delta\phi_{NL} = \beta P L / 2 = \beta P_{in} L / 4$  ( $P_{in}$  being the NOLM input power, and  $L$  the loop length) appears between the counterpropagating beams. Nonlinearity does not affect, however, the polarization orientation of these beams. Indeed, after crossing the QWP, the CCW beam enters the loop with linear polarization, which does not undergo NPR. Hence, the polarization evolution of the CCW beam through the loop is not modified with respect to the low-power case. In contrast, the CW beam enters the loop with circular polarization, which formally undergoes maximal NPR. This rotation has no effect however on the circular polarization state of the CW beam. As a consequence, in the nonlinear regime, the two beams remain linearly polarized and parallel at the NOLM output. The interference is no longer destructive, however, as the phase difference is now  $\Delta\phi = \pi + \Delta\phi_{NL}$ . The transmission  $T = P_{out} / P_{in}$  thus evolves sinusoidally with  $P_{in}$ , starting from a minimum  $T_{min} = 0$  for  $P_{in} = 0$ , and reaching its

first maximum  $T_{\max} = I$  when  $\Delta\phi_{NL} = \pi$ , i.e., for  $P_{in} = P_{\pi} = 4\pi/(\beta L) = 3\lambda A_{eff}/(\tilde{n}_2 L)$ , this value being the critical power.

Let us now consider that we rotate the QWP by an angle  $\alpha \neq 0$  (see Fig. 1). As the circularly polarized beams that cross the QWP in both directions are turned into linear polarizations at  $45^\circ$  with respect to the QWP axes, a rotation of the latter by  $\alpha$  causes these polarizations to rotate by  $\alpha$ , in the same direction as the QWP. After crossing the QWP, the CW beam passes through the coupler, and its orientation is maintained at the NOLM output. In contrast, the CCW beam exiting the QWP propagates along the fiber loop. Due to the spatial configuration of the loop, the polarization of the CCW beam performs during this propagation a  $180^\circ$  rotation around the  $y$  axis perpendicular to the plane of the NOLM (we discard here the rotation due to the optical activity introduced by fiber torsion, which is constant and does not modify the conclusions). As a result, the CCW beam appears at the NOLM output rotated by  $\alpha$ , but in the direction opposite to the CW beam. The polarization states of the counterpropagating beams are thus kept linear, but are no longer parallel for  $\alpha \neq 0$ . Hence, the purpose of the QWP is to adjust the polarization direction of the CW and CCW beams. If the QWP is rotated by  $\alpha$ , the angle between the orientations of the linearly polarized beams is  $2\alpha$ . Their interference is thus no longer complete, so that when the power (hence the nonlinear phase difference) is swept, the magnitude of the sinusoidal transmission variation is reduced: minimal transmission no longer reaches 0, nor  $I$  its maximal value. An extreme case appears for  $\alpha = \pi/4$ : the two polarization directions are then orthogonal at the NOLM output, and the beams do not interfere at all. As a consequence, independently of the input power value, and thus of the phase difference between the beams, the transmission is constant,  $T = 0.5$ . When  $\alpha = \pi/2$ , the polarization directions are again parallel, and the situation is very similar to the case  $\alpha = 0$ . In conclusion, the NOLM behavior is periodic in  $\alpha$ , with a period of  $\pi/2$ .

The results of Ref. 20 can be expressed in a simple analytical expression for the transmission of a NOLM made of highly twisted fiber and a QWP, in the case of circular input polarization. When the coupler is symmetrical, this expression is (taking  $\alpha = 0$  at minimal linear transmission):

$$T(P_{in}, \alpha) = \frac{P_{out}}{P_{in}} = \frac{1}{2} - \frac{1}{4} \left[ \cos\left(\pi \frac{P_{in}}{P_{\pi}}\right) + \cos\left(\pi \frac{P_{in}}{P_{\pi}} + 4\alpha\right) \right]. \quad (2)$$

This formula is in agreement with our analysis, and summarizes the above conclusions. For  $\alpha = 0$  ( $+k\pi/2$ ,  $k$  integer), the switching behavior of the NOLM is optimal for various applications. Indeed, thanks to the use of a symmetrical coupler, contrast is theoretically infinite, and as no additional loss was inserted in the loop, the NOLM insertion loss is zero, and the maximal transmission is equal to one (neglecting the loss introduced by the coupler and fiber loop). This design thus offers obvious advantages with respect to asymmetric-coupler-based schemes, where the coupling ratio limits the contrast, and to schemes including a loss element in the loop, because of the high insertion loss obtained in this case. Now, by a simple rotation of the QWP, the transmission can be made completely linear. Such a control on the switching characteristic is very interesting in practice. It has to be noted however that the validity of this description is strongly conditioned by the polarization states of the CW and CCW beams in the loop, which are ideally circular and linear, respectively. Indeed, if these beams show up some ellipticity (which happens for example if the input polarization is not exactly circular, or if the wave plate slightly differs from  $\lambda/4$ ), nonlinear ellipse rotation will take place at high power. Because of this extra rotation, the output polarization states will no longer keep a constant angle at the NOLM output. Their relative orientation, and not only their relative phase, will then depend on power, which is likely to degrade the optimal switching behavior described above. It is thus important to assess the validity of this simple model in real experimental conditions.

### 3. Experiment

We experimentally investigated the validity of Eq. (2). For this purpose, we used a NOLM (Fig. 2) made of 100 m of low-birefringence, highly twisted Corning SMF-28 standard fiber, which was fusion-spliced with the output ports of a nearly symmetrical fused coupler (coupling ratio  $r = 0.51$ ). High twist ( $q \approx 6$  turns/m) is applied to create strong optical activity (circular birefringence) in the fiber. This twist corresponds to a rotatory power  $\rho = \pi / \lambda (n_- - n_+) = hq / (2n) \approx 0.6\pi / m$  (with  $h \approx 0.13-0.16$  and the average index  $n = 1.45$  at  $\lambda = 1550$  nm), which means that the polarization state performs half a turn every 1.67 m. This distance has to be compared with the beat length  $L_B$  associated with the residual birefringence of the (untwisted) fiber, which was measured to be about 15 m for Corning SMF-28 [4]. Note that this value does not take into account stress-induced birefringence originating from the bending of the fiber, which was wrapped on a spool. Considering the spool diameter of 16.5 cm, we estimated the beat length resulting from this bending to be  $\sim 20$  m (for 125  $\mu\text{m}$  cladding diameter) [22]. Finally, we did not measure any significant residual optical activity in the Corning SMF-28 fiber, so that we believe that it is small compared with the twist-induced circular birefringence.

At one end of the spool, the fiber is wrapped on a small cylinder of properly chosen diameter, so as to form a QWP whose orientation can be adjusted [22]. We used as the input signal a 0.8-MHz train of sub-nanosecond optical pulses (duration  $\approx 0.2$  ns) generated by a figure-eight laser (1.55  $\mu\text{m}$ ,  $\sim 1$  mW average power). After passing through a mechanical chopper and an erbium-doped fiber amplifier (small-signal gain  $\approx 18.5$  dB), the pulses were circularly polarized using a polarizer and a polarization controller prior to the NOLM input. Through using a 0.99/0.01 coupler and  $\sim 100$  m of fiber, the input pulse was detected together with the corresponding output pulse, using two identical InGaAs photodetectors (1-GHz bandwidth). Both pulses were then monitored on a 2-channel oscilloscope (Tektronix TDS 3052, 500-MHz bandwidth) used in single shot mode (triggered off the input pulse). Varying the trigger level, input and output pulses were measured for various values of input power. The transmission was then obtained by making the ratio between output and input peak voltages. For a better estimation of input peak powers, a 20-GHz digital oscilloscope (Agilent Technologies 86100B infiniium DCA) was also used. Curves of the NOLM nonlinear transmission were obtained in this way for various values of the QWP angle. Finally, using the same setup, but reducing the pulse power and without chopper, the dependence of the linear (low-power) transmission with the QWP angle was obtained.

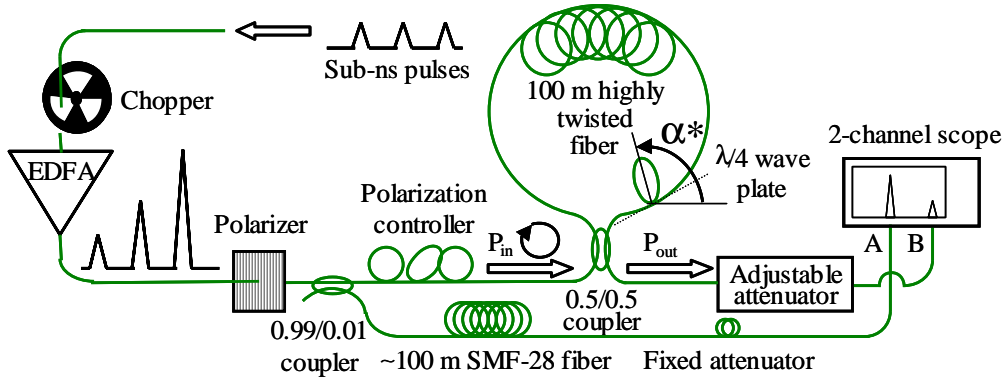


Fig. 2. Experimental setup.

Figure 3 shows the linear transmission against the QWP angle. Taking  $P_{in} = 0$ , Eq. (2) shows that the linear transmission is a sinusoidal function of  $\alpha$ , with a period of  $\pi/2$ . A

sinusoidal dependence is found experimentally, as can be seen in Fig. 3, with a period however superior to that predicted theoretically. This can be partly explained by the fact that, in the model, the QWP is independent of the fiber in the loop. In contrast, in the experiment, the QWP rotation twists the extremities of the fiber, which are connected to it. Hence, due to optical activity, if the QWP rotates by some angle, light polarization in both fiber ends is rotated by  $hq/(2n) \approx 5\%$  of this value in the same direction. As a result, an effect on the NOLM behavior expected for some value of the QWP rotation angle is actually observed for a larger angle. In other words, there is in theory a point-to-point equivalence between a fiber coil rotated by an angle  $\alpha^*$ , and a bulk wave plate rotated by  $\alpha = [1 - hq/(2n)]\alpha^* \approx 0.95\alpha^*$  [22].  $\alpha$  is thus the effective (theoretical) QWP angle, whereas  $\alpha^*$  is the angle measured experimentally. A better correspondence however between the model and the experimental data of Fig. 3 is obtained considering in Eq. (2) that  $\alpha \approx 0.86\alpha^*$ .

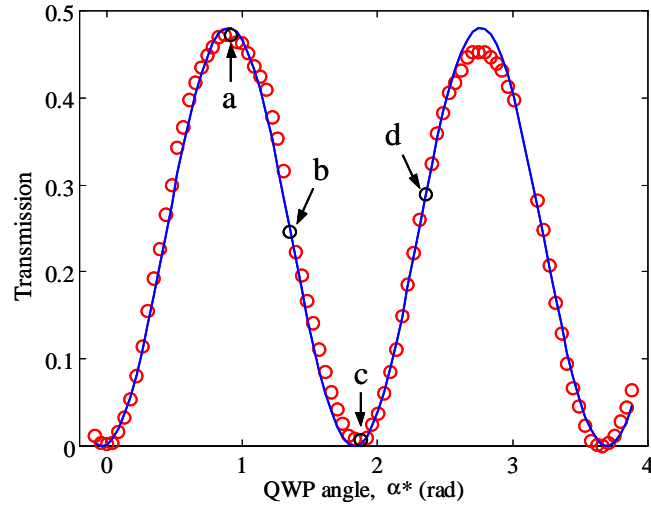


Fig. 3. Linear NOLM transmission versus quarter-wave plate angle  $\alpha^*$ . Circles: measured data; Solid line: sinusoidal fit.

We verified experimentally the validity of the nonlinear transmission given by Eq. (2) for different values of  $\alpha^*$ , corresponding in the linear regime to the points labeled *a* to *d* in Fig. 3. The four corresponding curves are presented in Fig. 4. Figure 4(a) was obtained for  $\alpha^* = 0.92$ , corresponding to the maximal linear transmission (point *a* in Fig. 3). At that position, the transmission shows no significant change with power, and remains close to 0.5. Indeed, using Eq. (2), maximal linear transmission,  $T = 0.5$ , is obtained for  $\alpha^* = 0.91$  ( $\alpha = \pi/4$ ). This value of the transmission is independent of power, as the cosine terms in Eq. (2) cancel out for  $\alpha = \pi/4$ . Through linear fitting of the data of Fig. 4(a), we obtained a nearly horizontal dependence, with  $T = 0.48$ , close to the theoretical value. For Fig. 4(b-d), we used directly Eq. (2) to fit experimental data, the optimization leading to best values of  $\alpha^*$  and  $P_\pi$  (the amplitude of the sinusoidal function was also slightly adjusted to improve the correspondence). Data of Fig. 4(b) were measured for  $\alpha^* = 1.35$  (point *b* in Fig. 3), and fitting led to  $\alpha^* = 1.30$ , and  $P_\pi = 131$  W. Figure 4(c) corresponds to minimal linear transmission, which was measured for  $\alpha^* = 1.88$  (point *c* in Fig. 3). The best fit was obtained for  $\alpha^* = 1.81$  (nearly corresponding to  $\alpha = \pi/2$ ), and  $P_\pi = 115$  W. Finally, in the case of Fig. 4(d),  $\alpha^* = 2.36$  (point *d* in Fig. 3), and the fit led to  $\alpha^* = 2.33$ , and  $P_\pi = 160$  W. It results from Fig. 4 that, in each case, Eq. (2) fits quite well the experimental results, for values of the QWP angle that are in good agreement with the angles at which the nonlinear



characteristics were actually measured. In addition, using the parameters of our experiment ( $\lambda = 1.55 \mu\text{m}$ ,  $A_{\text{eff}} = 80 \mu\text{m}^2$ ,  $\tilde{n}_2 = 3.2 \times 10^{-20} \text{ m}^2/\text{W}$  and  $L = 100 \text{ m}$ ), we find that  $P_\pi = 3\lambda A_{\text{eff}} / (\tilde{n}_2 L) = 116 \text{ W}$ . The values of the critical power determined for each QWP angle through fitting with Eq. (2) are quite compatible with this theoretical value, considering the precision of absolute power estimations.

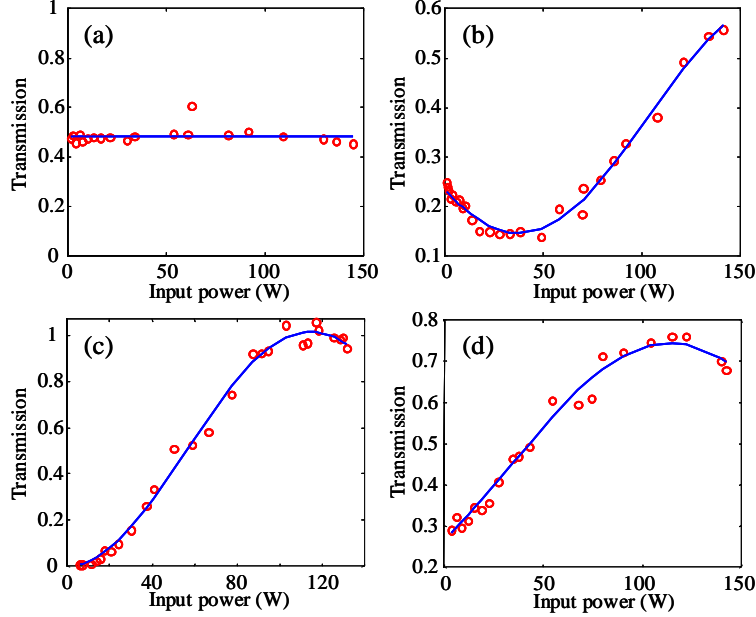


Fig. 4. NOLM transmission versus input power, for  $\alpha^* = 0.92$  (a),  $1.35$  (b),  $1.88$  (c), and  $2.36$  (d). Circles: measured data; Solid line: best fit.

From Fig. 4, it is clear that, except in the particular case of  $\alpha^* = 0.92$  (maximal linear transmission), a nonlinear dependence of the transmission exists, in spite of the use of a symmetrical coupler in the NOLM design. Switching with the highest contrast is observed for  $\alpha^* = 1.88$  [Fig. 4(c)]. In this case, similar to the case  $\alpha^* = 0$ , Eq. (2) shows that  $T_{\min} = 0$  for  $P_{\text{in}} = 0$ , and  $T_{\max} = 1$  for  $P_{\text{in}} = P_\pi$  (infinite contrast). Experimentally, data of Fig. 4(c) show that  $T_{\max} \approx 1$  and  $T_{\min} \approx 7 \times 10^{-3}$ , leading to a contrast  $C = T_{\max} / T_{\min} \approx 150$ . This nonzero value of  $T_{\min}$  is due to the residual asymmetry of the coupler ( $r = 0.51$ ), as well as to the fact that point  $c$  in Fig. 3 only corresponds approximately to minimal linear transmission. Adjusting more accurately the QWP angle, the value of  $T_{\min}$  is limited only by the coupler asymmetry, and we have  $T_{\min} = (1 - 2r)^2 = 4 \times 10^{-4}$  for  $r = 0.51$ . The contrast of the switching characteristic obtained in this case is  $C = 2500$ . Such values of the contrast were found experimentally. With a value of  $r \neq 0.5$ , power imbalance obviously plays some role in the NOLM switching. This role is minor however for  $r = 0.51$ . If we discard polarization-induced nonlinear effects, the critical power is given by [8]  $P_\pi = \lambda A_{\text{eff}} / [2\tilde{n}_2 L |2r - 1|]$ , which leads to  $P_\pi = 969 \text{ W}$  using parameters of our NOLM. This value of  $P_\pi$  is clearly incompatible with those reported here, which demonstrates the crucial importance of considering the polarization asymmetry to describe the NOLM operation.

In this experiment, rather long ( $\sim 0.2 \text{ ns}$ ) pulses were used. For ultrafast photonic applications however, picosecond pulses must be used, and in this case some deviation is expected from the NOLM operation as described here. This is due in particular to the group-

velocity mismatch that appears in a twisted fiber between both circular polarization components, and which is characterized by  $\delta = \Delta n / c$ , where  $\Delta n = \lambda / \pi \times hq / (2n)$ . With the parameters of our experiment, we find that  $\delta \approx 3$  fs/m. Hence, after propagation down the fiber ( $L = 100$  m), both polarization components of the pulses are separated by  $\delta L \approx 0.3$  ps. As a consequence, we believe that the continuous-wave approach that is proposed here can be used to describe accurately the operation of our set-up for pulses down to about 5 ps in duration. For shorter pulses, group-velocity mismatch can no longer be ignored for a reliable quantitative description of the NOLM operation. A model that encompasses this effect must consider the time-varying envelope of the signal, and this kind of problem in general can be investigated only numerically (the same observation is valid if the effects of dispersion are included). We thus believe that the present description will constitute a basis for future investigations for the design of efficient ultrafast photonic devices.

#### 4. Conclusion

In conclusion, we analyzed the operation of a NOLM made of a symmetrical coupler, highly twisted fiber and a QWP located asymmetrically in the loop. We proposed a simple description of the NOLM behavior, showing that nonlinear switching is obtained through the polarization asymmetry generated by the QWP. Our analysis also emphasizes some of the advantages of the proposed architecture over classical NOLM designs. These include a high contrast while maintaining low critical power and low insertion loss, as well as an easy adjustment procedure. Indeed, the device can be tuned continuously from power-independent transmission to complete switching operation simply by adjusting the QWP angle. This procedure is much more convenient than the blind tuning of a polarization controller, a method commonly used in most conventional NOLM designs. Our analysis also pointed out that the outstanding properties of this NOLM are conditioned by the actual polarization states of the beams that propagate in the loop. We characterized experimentally the NOLM transmission, for various values of the QWP angle. As the experimental results are in good agreement with theoretical predictions, we conclude that our model is valid in real laboratory conditions. For any value of the input power, the slope of the transmission can be modified, canceled or inverted by tuning the QWP angle. Given the decisive advantages presented by this novel structure compared with conventional NOLM designs, and considering the wide spectrum of applications where NOLMs are found today, we believe that the proposed design will play an important role in future ultrafast photonic systems.

#### Acknowledgments

O. Pottiez is supported by CONACyT (Mexican Council for Science and Technology), by F.N.R.S. (Belgian Fund for Scientific Research) and by the Interuniversity Attraction Pole IAP V/18 program of the Belgian Science Policy. This work was also funded by CONACyT project J36135-A. The authors would like to thank J. W. Haus for fruitful discussions and careful reading of the manuscript.